ACS OMEGA

http://pubs.acs.org/journal/acsodf

Article

Pyridine- and Thiazole-Based Hydrazides with Promising Anti-inflammatory and Antimicrobial Activities along with Their *In Silico* Studies

Vinuta Kamat, Rangappa Santosh, Boja Poojary,* Suresh P. Nayak, Banoth Karan Kumar, Murugesan Sankaranarayanan, Faheem, Sheela Khanapure, Delicia Avilla. Barretto, and Shyam K. Vootla

Cite This: *ACS Omega* 2020, 5, 25228−25239

Read Online

ACCESS | Metrics & More | Article Recommendations | Supporting Information

ABSTRACT: A new class of compounds formed by the linkage of −C(O)−NH− with pyridine and thiazole moieties was designed, synthesized, and characterized by various spectral approaches. The newly characterized compounds were evaluated for their antimicrobial as well as anti-inflammatory properties. The *in vitro* anti-inflammatory activity of these compounds was evaluated by denaturation of the bovine serum albumin method and showed inhibition in the range of IC_{50} values—46.29−100.60 μg/mL. Among all the tested compounds, compound **5l** has the highest IC_{50} value and compound **5g** has the least IC_{50} value. On the other hand, antimicrobial results revealed that compound **5j** showed the lowest MIC values and compound **5a** has the highest MIC values. Furthermore, molecular docking of the active compounds demonstrated a better docking score and interacted well with the target protein. Physicochemical parameters of the titled compounds were found suitable in the reference range only. The *in silico* molecular docking study revealed their COX-inhibitory action. Compound **5j** emerged as a significant bioactive molecule among the synthesized analogues.

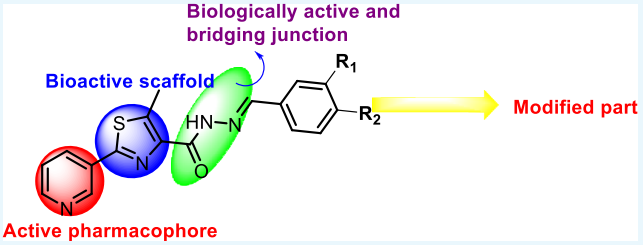

INTRODUCTION

Inflammation is provoked by injuring any tissue in the body or by infection through pathogens, such as bacteria and viruses, allergens, irritants, toxic compounds, and so forth, either exogenously or endogenously.[1] This may also include injury, surgery, autoimmune disorder, adult respiratory distress syndrome, long-term exposure to industrial chemicals, and reoxygenation injuries. The inflammation process is catalyzed by easily accessible molecules in the body such as histamine, prostaglandins, leukotrienes, oxygen- and nitrogen-derived free radicals, serotonin, bradykinin, and interleukins. Extravagant inflammation may lead to stroke or heart diseases, lupus, cancer, tissue injury, physiological decompensation, organ damage, and death.[2] The risks associated with the inflammation process pose a challenge to the medicinal chemists to search for more effective anti-inflammatory agents. A majority of the existing anti-inflammatory compounds, especially those with proven clinical efficiency, are acidic in nature, such as aspirin, indomethacin, flufenamic acid, ibuprofen, and so forth. Nonsteroidal anti-inflammatory drugs (NSAIDs) that act on the affected tissues[3,4] by inhibiting the cyclooxygenase (COX) involved in the synthesis of prostaglandins are one of the major class of drugs used to treat inflammation.[5−9]

Various natural as well as synthetic compounds containing the thiazole core moiety have been explored for their antitumor,[10,11] antimicrobial, anti-HIV,[12] anticoagulant,[13] anti-inflammatory,[14] and antioxidant[15] properties since many decades. The available literature also supports the bioactivities of thiazole scaffolds (Figure 1).

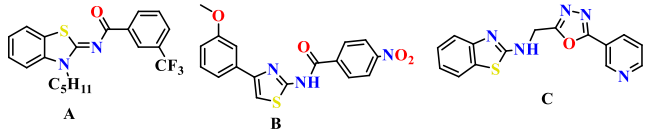

Figure 1. Structure of thiazole-based molecules as anti-inflammatory agents.

Compound **A** demonstrated its selective cannabinoid CB2 agonists with anti-inflammatory activity.[16] Compound **B** is a thiazole derivative exhibiting anti-inflammatory property,[17] and compound **C** is a 1,3,4-oxadiazole-benzothiazole-pyridine conjugate which showed promising COX inhibition.[18]

In recent decades, microbial infections are widespread and one of the life-threatening problems. To overcome these situations, researchers are trying hard to discover more efficient

Received: July 15, 2020
Accepted: September 4, 2020
Published: September 25, 2020

https://dx.doi.org/10.1021/acsomega.0c03386
ACS Omega 2020, 5, 25228−25239

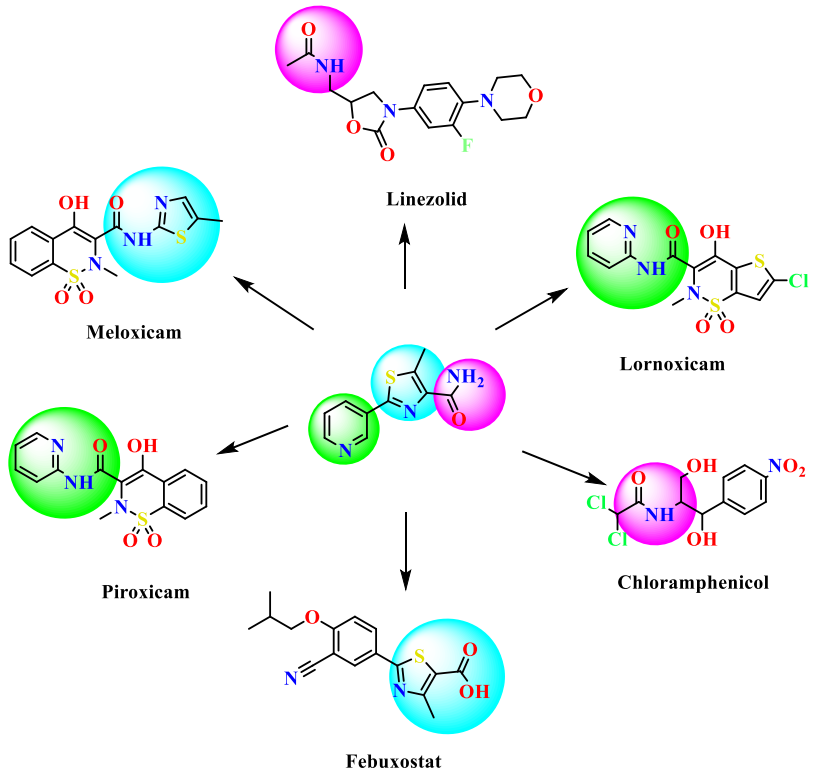

Figure 2. Structure of pyridine-, thiazole-, and amide-containing bioactive molecules.

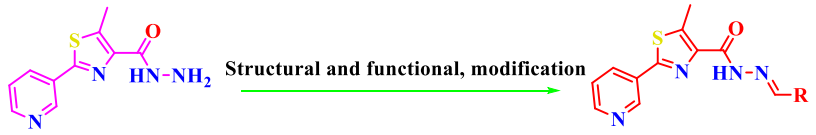

Figure 3. Strategy used in designing the titled molecules.

and effective antimicrobial candidates against both drug-sensitive as well as drug-resistant strains. Mahmoud *et al.*,[19] Adole *et al.*,[20] Wang *et al.*,[21] and Eryılmaz *et al.*[22] reported various thiazole containing antimicrobial candidates. Some of the known reported bioactive compounds containing pyridine and thiazole having amide linkages are shown in Figure 2. Based on the available literature, the thiazole nucleus has been considered as one of the promising bioactive scaffolds in the wide range of biological systems.

Various pyridine containing anti-inflammatory and antimicrobial agents are also reported in the literature. Researchers like Fan *et al.*,[23] Bhila *et al.*,[24] Desai *et al.*,[25] Rani and Reddy,[26] and Rashdan *et al.*[27] reported some antimicrobial agents. Laddha and Bhatnagar,[28] Kumar *et al.*,[29] and Thirumurugan *et al.*[30] reported some pyridine-based anti-inflammatory agents. In view of these observations,[31] we also aimed to synthesize some hydrazides linked to pyridine-containing thiazole as potent bioactive scaffolds. The strategy used in this study is presented in Figure 3.

Scheme 1. Synthetic Pathway of the Thiazole-Based Hydrazides (5a–l)[a]

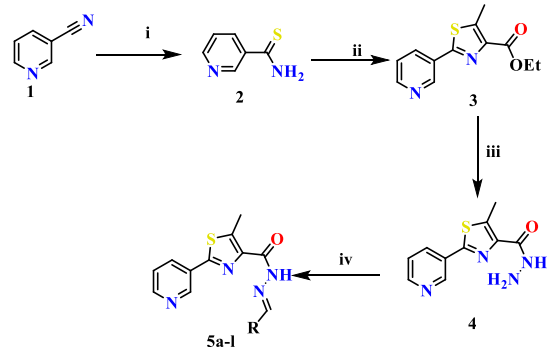

[a]Reagents: (i): P_4S_{10}, ethanol, reflux, 70 °C, 4 h; (ii): ethyl 2-chloroacetoacetate, ethanol, reflux, 70 °C, 8 h; (iii): hydrazine hydrate, ethanol, reflux, 70 °C, 4 h; (iv): Ar-CHO, ethanol, reflux, 70 °C, 12 h.

RESULTS AND DISCUSSION

Chemistry. The detailed synthetic strategy for the target compounds is illustrated in Scheme 1. The structures and the yield of the synthesized compounds are represented in Figure 4. Initially, 3-cyanopyridine (1) was converted to pyridine-3-carbothiamide (2) by treating with P_4S_{10}. Compound **2** upon refluxing with ethyl-2-chloroacetoacetate resulted in ethyl-5-methyl-2-(pyridine-3-yl)thiazole-4-carboxylate (3). The resulting ester was treated with hydrazine hydrate to yield 5-methyl-2-(pyridine-3-yl)thiazole-4-carbohydrazide (4). Further, 5-methyl-2-(pyridine-3-yl)thiazole-4-carbohydrazide was condensed with an aromatic aldehyde to afford the target compounds (**5a–l**). The formation of **5a–l** was confirmed by the absence of IR bands around 3330 cm^{-1} and scissoring at

https://dx.doi.org/10.1021/acsomega.0c03386
ACS Omega 2020, 5, 25228−25239

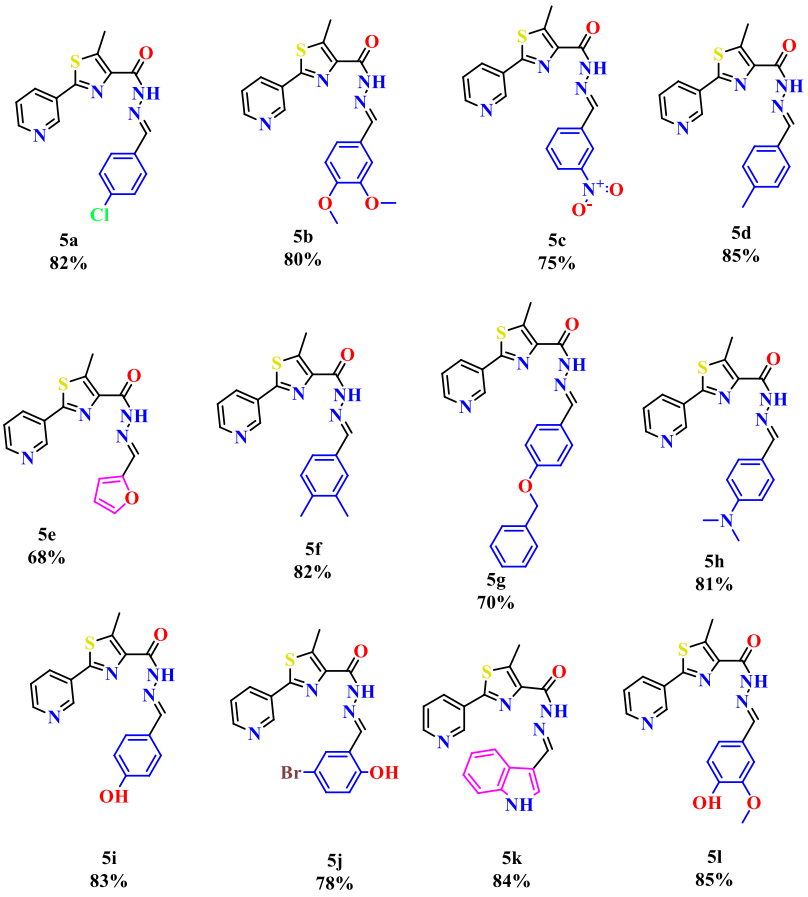

Figure 4. Structure of the synthesized compounds.

Table 1. Percentage Inhibition of Egg Albumin Protein Denaturation by the Synthesized Compounds[a]

	inhibition of protein denaturation (%)												
con (μg/mL)	std*	5a*	5b*	5c*	5d*	5e*	5f*	5g*	5h*	5i*	5j*	5k*	5l*
20	42.98 ± 1.28	11.66 ± 0.95	22.66 ± 1.05	12.76 ± 0.99	24.46 ± 1.19	28.63 ± 0.68	17.65 ± 1.34	9.94 ± 0.53	19.18 ± 0.71	25.49 ± 0.85	30.66 ± 1.04	31.42 ± 0.95	**32.63 ± 1.07**
40	57.08 ± 1.6	20.51 ± 0.82	30.51 ± 2.22	22.51 ± 2.33	35.06 ± 0.56	39.23 ± 1.37	27.27 ± 1.52	16.82 ± 1.74	27.92 ± 1.59	31.18 ± 1.28	40.01 ± 1.33	41.00 ± 1.24	**43.20 ± 1.87**
60	75.54 ± 1.26	28.25 ± 1.47	42.86 ± 2.43	28.91 ± 1.44	48.94 ± 1.53	51.18 ± 1.26	35.26 ± 1.42	26.00 ± 1.00	37.33 ± 1.43	49.24 ± 1.60	53.98 ± 1.78	56.72 ± 2.00	**59.51 ± 2.46**
80	83.56 ± 0.96	39.55 ± 0.92	52.54 ± 0.90	39.65 ± 1.08	61.43 ± 1.24	65.57 ± 1.33	49.58 ± 0.98	37.61 ± 1.99	49.89 ± 1.45	58.12 ± 0.56	68.39 ± 1.00	71.47 ± 0.90	**78.24 ± 1.37**
100	94.60 ± 0.90	52.56 ± 0.80	69.65 ± 1.21	58.28 ± 1.29	73.82 ± 1.45	77.37 ± 0.94	62.06 ± 1.57	49.70 ± 0.73	65.78 ± 1.64	71.07 ± 0.34	80.34 ± 0.95	83.46 ± 2.21	**87.97 ± 1.37**
IC_{50} μg/mL	35.03	95.11	76.12	85.79	61.29	58.62	80.68	100.60	80.18	62.74	55.58	52.89	**46.29**

[a]Values are expressed as mean ± SD, n = 3, and * Correlation is significant at the 0.01 level.

1589 cm^{-1} due to the NH_2 group and the presence of CH stretching at 2860 cm^{-1}. A singlet at δ 8 ppm confirmed the formation of −CH═N.

Biological Activity. *In Vitro Anti-inflammatory Activity (Denaturation of the Bovine Serum Albumin Method).* Inflammation is the biological response that takes place when the healthy tissues get damaged or injured by harmful pathogens or by the alteration of neighboring protein tissues. Because of the lack of groundwork, animal risk management, and ethical disputes, *in vivo* studies have potential complications in order to carry out the animal studies. The leading cause of inflammation is the alteration of the native state of the tissue proteins. In the *in vivo* studies, the denaturation of proteins takes place because of the synthesis of autoantigens, and the compounds which inhibit denaturation are potentially useful for the discovery of novel anti-inflammatory drugs. The inhibitory effect on denaturation of proteins can be accessed by using a heat-induced protein denaturation process using diclofenac sodium as the standard drug. For the protein denaturation process to take place, the main important property to be maintained in several NSAIDs evaluation is the physiological pH (6.2−6.5) range of the reaction medium. All the synthesized thiazole-based hydrazide derivatives were tested for their *in vitro* anti-inflammatory activity by inhibition of the protein (bovine albumin) denaturation method using diclofenac sodium as a standard drug. Percentage inhibition of

https://dx.doi.org/10.1021/acsomega.0c03386
ACS Omega 2020, 5, 25228−25239

the synthesized compounds was determined using varying concentrations that is, 20−100 μg/mL. The IC_{50} values were determined, and the results and graphical representations are tabulated in Table 1 and Figure 5, respectively. From the

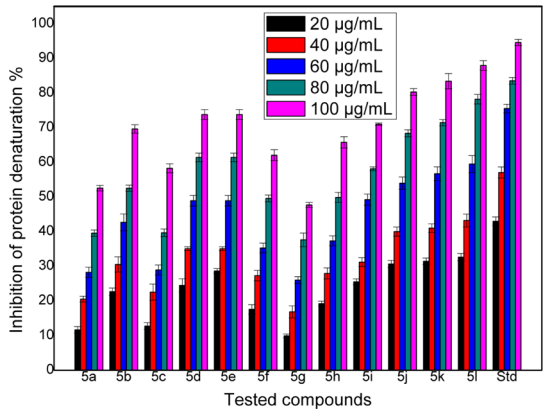

Figure 5. Graphical representation of *in vitro* protein denaturation results of the compounds.

results, it is clear that some of the synthesized compounds showed better activity (compounds **5j**, **5k**, and **5l**). IC_{50} values of the synthesized compounds were in the range of 46.29−100.60 μg/mL because of the structural variations of the substrate. By varying the substitutions, the potency of the compounds changed. Compound **5l** has the highest inhibition among the synthesized compounds which have 4-hydroxy-3-methoxyphenyl, and it has more inhibition than **5b** (which has 3,4-dimethoxy substitution) and **5i** (which has a hydroxyl group at 4th position). The lowest inhibition was observed for **5g**, which has the 4-benzyloxyphenyl group. The compounds containing heterocyclic rings, **5k**, and **5e** showed better inhibition when compared with the compounds having aromatic substituents such as **5a**, **5c**, and **5g**. Compounds **5b**, **5d**, **5f**, **5h**, and **5i** (3,4-dimethoxy, 4-methyl, 3,4-dimethyl, 4-*N*,*N*-dimethyl, and 4-hydroxy) showed moderate inhibition. It can be concluded finally that the presence of the hydroxyl group on the phenyl ring and/or the presence of heterocyclic moieties exhibit good inhibition.

The structure activity relationship study of the active compound **5l** was deduced based on the IC_{50} value; it clearly reveals that the presence of hydroxyl and methoxy groups is responsible for the enhanced inhibition. The presence of the hydroxyl substituent on the 4th place and the methoxy substituent on the 3rd position enhanced the anti-inflammatory activity drastically.

In Vitro Antimicrobial Activity. Minimal inhibitory concentration of the synthesized compounds showed the highest to least values because of the structural modifications of the substrate. Minimal inhibitory concentration values along with mean ± SD and graphical representations of antibacterial and antifungal activities are tabulated in Tables 2 and 3 and in Figures S11 and S12, respectively.

The variation of the position of the substituents and the introduction of the heterocyclic ring were explored to study the structure−activity relationship (SAR) of the synthesized compounds. Results obtained from the antimicrobial studies indicated that the compounds **5j**, **5k**, **5l**, **5e**, and **5i** showed significant minimal inhibitory concentration (MIC) values, of which the compound **5j** showed MIC values as that of the standard drugs against the tested bacterial and fungal strains. The enhanced antimicrobial activity is due to either the presence of a hydroxyl group on the aromatic ring and or the presence of the heterocyclic moiety in the synthesized derivatives when compared with other compounds having the aromatic moiety. The least activity was shown by compounds **5a**, **5b**, and **5c** with 4-chloro, 3,4-dimethoxyphenyl, and 3-nitrophenyl moieties, respectively. The moderate antimicrobial property was observed in the case of compounds **5f**, **5d**, **5g**, and **5h**, which contain 3,4-dimethyl, 4-methyl, and 4-benzyloxyphenyl groups.

The structural activity relationship study deduced that the alterations in the aryl ring play the significant role for enhancing the activity. Compound **5j** with the combinations of bromo substitution at the 5th position and hydroxyl substitution at the 2nd position produces effective and enhanced antimicrobial properties.

In silico prediction of physicochemical and ADME parameters: in the field of medicinal chemistry, Lipinski's rule of five and Veber's rule are the guidelines for medicinal chemists searching drug-like chemical compounds with effective oral potential. It is understood that fine-tuning the physicochemical properties (PCPs) of a lead molecule could alter the ADME property. Hence, close inspection was placed

Table 2. MIC Values (μg/mL) of Antibacterial Evaluation of the Titled Compounds[a]

compound	*S. aureus*	*B. subtilis*	*E. coli*	*P. aeruginosa*
5a	127.66 ± 1.52	127.33 ± 1.15	128.33 ± 0.57	127.33 ± 1.15
5b	127.00 ± 1.73	65.00 ± 1.73	128.33 ± 0.57	127.00 ± 1.73
5c	64.00 ± 1.00	32.66 ± 1.15	64.33 ± 0.57	64.00 ± 1.00
5d	63.00 ± 1.00	31.66 ± 0.57	65.00 ± 1.00	64.33 ± 1.52
5e	15.66 ± 0.57	8.33 ± 0.57	17.33 ± 1.52	16.00 ± 1.00
5f	33.00 ± 1.73	15.33 ± 1.15	31.66 ± 1.52	31.33 ± 1.15
5g	63.66 ± 0.57	33.00 ± 1.73	64.66 ± 1.15	64.00 ± 1.00
5h	31.66 ± 0.57	17.00 ± 1.73	32.66 ± 1.15	32.00 ± 2.00
5i	15.33 ± 1.15	7.00 ± 1.00	17.00 ± 1.00	16.33 ± 0.57
5j	**1.66 ± 0.57**	**1.32 ± 0.57**	**2.66 ± 1.52**	**2.33 ± 0.57**
5k	3.66 ± 1.52	2.00 ± 1.00	4.66 ± 1.15	4.00 ± 1.00
5l	4.00 ± 01.73	4.33 ± 0.57	7.00 ± 1.00	7.00 ± 1.00
tetracycline	0.68 ± 0.54	0.66 ± 0.28	1.66 ± 1.15	1.66 ± 1.15
streptomycin	1.00 ± 00	1.00 ± 00	1.66 ± 1.15	1.00 ± 0.86

[a]Values are expressed as mean ± SD, n = 3, and * correlation is significant at the 0.01 level.

https://dx.doi.org/10.1021/acsomega.0c03386
ACS Omega 2020, 5, 25228−25239

Table 3. MIC Values (μg/mL) of Antifungal Evaluation of the Titled Compounds[a]

compound	*A. flavus*	*T. atroviridae*	*P. citranum*	*C. albicans*
5a	126.33 ± 2.08	126.00 ± 1.73	124.33 ± 2.30	128.33 ± 0.57
5b	128.33 ± 2.08	129.00 ± 2.00	124.00 ± 1.00	126.00 ± 2.00
5c	129.00 ± 1.73	127.33 ± 1.15	126.66 ± 2.30	62.33 ± 1.52
5d	64.00 ± 1.00	65.66 ± 1.52	67.00 ± 2.64	32.00 ± 1.00
5e	16.66 ± 1.15	15.66 ± 2.51	16.33 ± 1.52	8.33 ± 1.52
5f	32.66 ± 3.05	33.33 ± 1.52	32.00 ± 1.00	14.33 ± 1.52
5g	63.33 ± 1.15	62.66 ± 1.52	65.00 ± 1.73	130.33 ± 2.08
5h	64.6 ± 3.05	65.00 ± 1.73	65.33 ± 1.52	33.66 ± 2.08
5i	14.66 ± 2.30	15.00 ± 1.73	15.33 ± 1.15	7.66 ± 1.52
5j	**2.66 ± 1.15**	**2.33 ± 0.57**	**1.66 ± 0.57**	**1.66 ± 1.15**
5k	3.00 ± 1.00	5.33 ± 1.52	4.66 ± 1.15	3.33 ± 1.52
5l	3.00 ± 1.00	5.33 ± 1.52	3.66 ± 1.52	4.00 ± 2.00
fluconazole	2.00 ± 0.00	2.00 ± 0.00	2.00 ± 0.00	1.00 ± 0.00
nystatin	3.33 ± 1.52	1.66 ± 1.15	2.00 ± 1.73	3.66 ± 2.08

[a]Values are expressed as mean ± SD, n = 3, and * correlation is significant at the 0.01 level.

Table 4. *In silico* Predicted Physicochemical Parameters of the Titled Compounds

code	MW[a]	SASA[b]	donorHB[c]	acceptHB[d]	log P o/w[e]	PCaco[f]	log S[g]	#rotor[h]	% human oral absorption[i]
5a	356.829	649.025	1	5.5	3.973	1059.54	−5.876	4	100
5b	382.436	705.878	1	7	3.667	839.026	−5.698	6	100
5c	367.381	671.77	1	6.5	2.701	91.567	−5.446	5	77.874
5d	336.411	663.689	1	5.5	3.875	951.014	−5.852	4	100
5e	312.345	571.87	1	6	2.687	976.977	−4.332	4	96.192
5f	350.437	689	1	5.5	4.093	982.991	−7.296	4	100
5g	428.508	788.776	1	6.25	5.283	1154.27	−4.073	7	100
5h	365.452	700.173	1	6.5	3.836	958.45	−6.293	5	100
5i	338.383	600.548	2	6.25	2.442	247.973	−5.946	5	84.098
5j	417.279	619.16	2	6.25	3.392	927.915	−6.187	5	100
5k	361.42	686.978	2	5.5	3.752	529.314	−5.307	4	100
5l	368.409	682.421	2	7	2.926	313.646	−4.982	6	88.762

[a]Molecular weight, in Da (range for 95% of drugs: 130−725 Da). [b]Total solvent-accessible volume in cubic angstroms using a probe with a 1.4 Å radius. (500−2000). [c]No. of hydrogen bonds donated by the molecule (range for 95% of drugs: 0−6). [d]No. of hydrogen bonds accepted by the molecule (range for 95% of drugs: 2−20). [e]Predicted octanol/water partition coefficient log P (acceptable range: −2.0 to 6.5). [f]Predicted aqueous solubility; S in mol/L (acceptable range: −6.5 to 0.5). [g]Apparent Caco-2 permeability (nm/s) (<25 poor, >500 great). [h]Number of nontrivial (not CX3) and nonhindered (not alkene, amide, small ring) rotatable bonds. (0−15). [i]% human oral absorption (>80 high and <25 poor).

on the PCPs, by calculating the guiding parameters such as molecular weight (MW), number of hydrogen bond acceptors (HBAs), number of hydrogen bond donors (HBDs) calculated log P (clog P), number of rotatable bonds (NRBs), and polar surface area (PSA). Compounds with optimal PCPs (MW < 500, HBA < 10, HBD < 5, log P < 5, NRB < 10, and PSA < 140 Å) have higher probability for oral absorption. The predicted parameters of the titled compounds (Table 4) satisfied the Lipinski's rule of five. Caco-2 permeability of all the predicted compounds lies within the range except compound **5c**, which showed a less permeability of 91.567 nm/s. 50% of the compounds revealed the predicted results of 100% oral human absorption, and the rest of the compounds exhibited the values within the range of 77−96%. Overall, the predicted parameters of the compounds were satisfied with the physicochemical parameters, which are exhibited by most of the clinically approved drugs. Based on the prediction studies, these compounds may not face any problems in the mere future.

Molecular Docking Studies. To find out the putative binding mode of the significantly active compound against the targeted protein COX-2, docking studies were performed. Before the docking studies of the test compound, root mean square deviation (RMSD) of the X-ray pose and redocked pose (Figure 6) of the co-crystallized ligand in the target protein was checked and found to be 0.20 Å, suggesting that the docking protocol could be relied on for the docking studies.

In-depth scrutiny of the 3D and 2D poses of the co-crystal ligand (Celecoxib) was performed (Figures 7 and 8), and celecoxib unveiled four hydrogen bond interactions within the target with a highest docking score of −12.4 kcal/mol and energy of −62.50 kcal/mol (5). The amino acid residues such as GLN-178, SER-339, ARG-499, and PHE-504 were actively involved in the hydrogen bond formation with celecoxib. Apart from the hydrogen bond interaction, celecoxib also revealed two aromatic bond interactions with the amino acid residues HIS-75 and TYR-341; ARG-106 was involved in $\pi-\pi$-cationic interaction with the pyrazole moiety of celecoxib.

Similarly, significantly active compound **5j** (Figures 9 and 10) also exhibited only one aromatic bond interaction with the amino acid residue SER-516 through the pyridine moiety. The compound exhibited a docking score of −9.80 kcal/mol and docking energy of −46.80 kcal/mol, which are comparatively less than those of the standard drug celecoxib.

https://dx.doi.org/10.1021/acsomega.0c03386
ACS Omega 2020, 5, 25228−25239

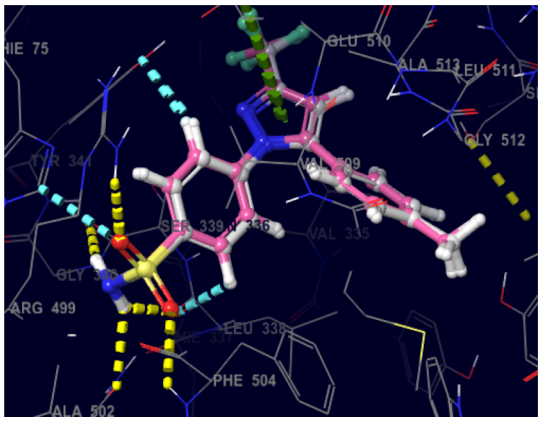

Figure 6. Superimposed view of the X-ray native pose of the ligand (Celecoxib) with its docking pose in the active site of the target (PDB-3LN1) [color interpretation: white—X-ray native pose of the ligand, pink—docked pose of the ligand].

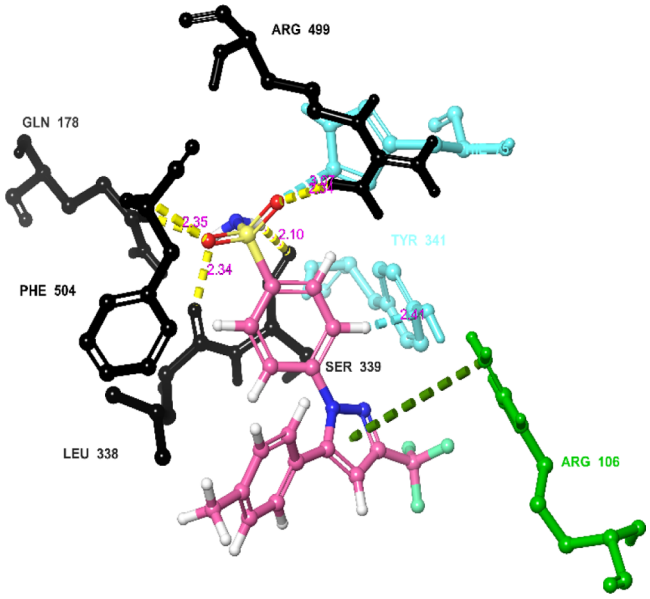

Figure 7. Networking of the co-crystal ligand exhibited various interactions in the active site of the protein (3LN1) [color interpretation: black—hydrogen bond, blue—aromatic bond, green—π–π cation interactions].

CONCLUSIONS

In the present study, we developed thiazole-based hydrazides as anti-inflammatory and antimicrobial agents. The *in vitro* anti-inflammatory study of the target compounds revealed that compounds **5j**, **5k**, and **5l** are significant inhibitors among the series. The *in vitro* antimicrobial assay showed that compounds **5j**, **5k**, and **5l** are effective against all the tested strains. The phenolic group, along with methoxy or bromo substituents, showed better activity when compared with other substituents. Compounds **5j** and **5l** displayed better activity in the series. Therefore, compounds **5j** and **5l** can be used for further studies. Pharmacokinetic studies also underlined that the active compound has better absorption, distribution, metabolism, and elimination profiles. More interestingly, compounds **5j**, **5k**, and **5l** showed significant biological activity with safe pharmacokinetic properties. The molecular docking study also supports the effective interactions with target molecules. Based on the present study, we can conclude that this is the potential route for the development of new effective antimicrobial as well as anti-inflammatory agents.

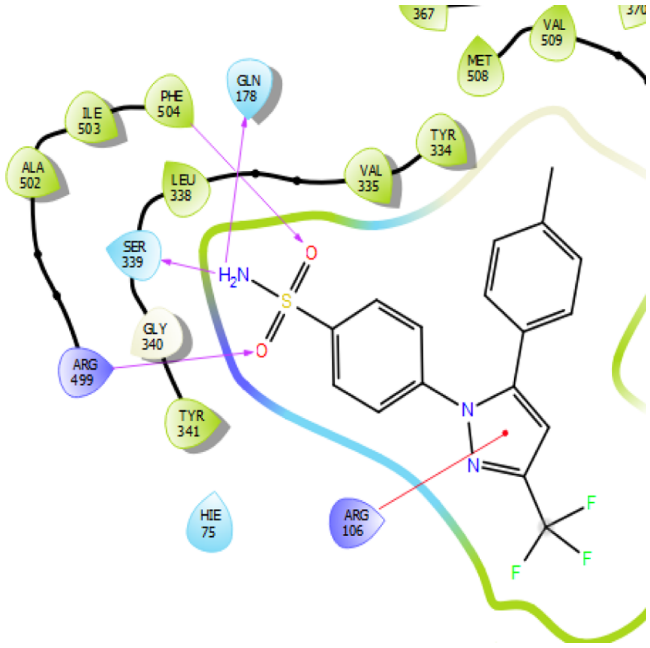

Figure 8. 2D representation of the co-crystal ligand [color interpretation: magenta—hydrogen bond, red—cation interactions.

EXPERIMENTAL SECTION

Materials and Methods. All the chemicals and solvents used for the present study were purchased from commercial suppliers of Sigma-Aldrich, India, and Spectrochem Pvt. Ltd., India, and used without purification. Reactions were carried out using standard techniques. Melting points of the newly synthesized compounds were determined in an open capillary tube and were uncorrected. To monitor the progress of the reaction and purity of the product, thin layer chromatography (Merck silica gel 60 F254-coated aluminum plates) was used. The mixture of ethyl acetate and hexane solvents was used as the mobile phase and visualized under UV light at 254 nm. Shimadzu-FTIR was used to record FTIR spectra (γ_{max} in cm^{-1}). The Bruker AVANCE II 400 spectrometer (with 5 mm PABBO BB-1H tubes) was used to record NMR spectra, using DMSO-d_6 as a solvent and TMS as an internal standard (the chemical shift in δ ppm and coupling constants (J) were expressed in parts per million (ppm) and hertz, respectively). VARIOEL-III (Elementar analysensysteme GmBH) was used for the elemental analysis.

Procedure for the Synthesis of Pyridine-3-carbothiamide (2). A solution of P_4S_{10} (2 equiv) and 3-cyanopyridine 1 (1 equiv) in ethanol was taken in a round-bottomed flask and stirred for 30 min at ambient temperature. The reaction mixture was then refluxed for 4 h. After the completion of the reaction [monitored by TLC (EtOAc/hexane 3:7)], the reaction mixture was cooled to room temperature, diluted with cold water, and extracted with chloroform (3 × 200 mL). The combined organic extract was dried over $CaCl_2$ and concentrated to dryness. Further, the crude residue was recrystallized to afford a pure compound.[32]

Procedure for the Synthesis of Ethyl-5-methyl-2-(pyridine-3-yl)thiazole-4-carboxylate (3). A mixture of

https://dx.doi.org/10.1021/acsomega.0c03386
ACS Omega 2020, 5, 25228−25239

Table 5. Docking Analysis of Celecoxib and Significantly Active Compounds 5j, 5k, and 5l

compound code				Glide score (kcal/mol)	
5j				−9.80	
5k				−7.80	
5l				−7.10	
code (PDB-3LN1)	H-bond	aromatic bond	$\pi-\pi$ interactions	Glide score (kcal/mol)	Glide energy (kcal/mol)
co-crystal ligand (Celecoxib)	GLN-178 SER-339 ARG-499 PHE-504	HIS-75 TYR-341		−12.40	−62.50
5j		SER-516		−9.80	−46.80

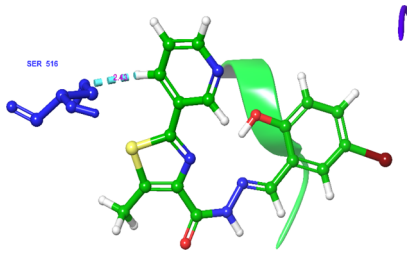

Figure 9. Networking of the significantly active compound 5j exhibited various interactions in the active site of the protein (3LN1) [color interpretation: blue—aromatic bond].

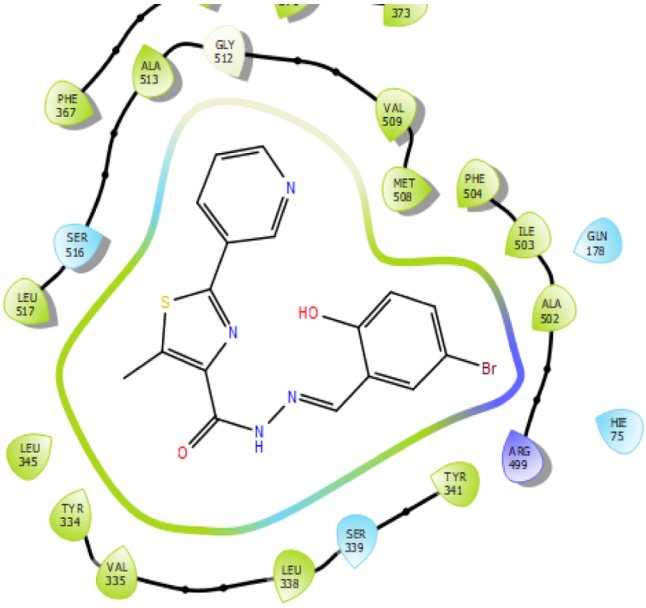

Figure 10. 2D representation of the significantly active compound 5j.

ethyl-2-chloro acetoacetate (1.2 equiv) and compound 2 (1 equiv) dissolved in ethanol (50 mL) was refluxed for 8 h. After completion of the reaction [monitored by TLC (EtOAc/hexane 3:7)], the reaction mixture was cooled to ambient temperature. The reaction mixture was quenched with ice cold water. The solids precipitated out were collected by filtration, washed with ice cold water, and dried under reduced pressure to afford intermediate 3.[33]

Procedure for the Synthesis of 5-Methyl-2-(pyridine-3-yl)thiazole-4-carbohydrazide (4). To the stirred solution of intermediate compound 3 (1.5 equiv) in ethanol (50 mL), hydrazine hydrate (2.5 equiv) was added at ambient temperature and heated to reflux for 4 h. The reaction progress was monitored by TLC (EtOAc/hexane 3:7). After completion of the reaction, the reaction mass was poured onto crushed ice and stirred for half an hour. The solid was filtered and dried under vacuum to get intermediate compound 4.[34]

General Procedure for the Synthesis of *N*′-Arylmethylidene-5-methyl-2-(pyridin-3-yl)thiazole-4-carbohydrazides (5). A mixture of intermediate compound 4 (1 equiv) and aromatic aldehyde (1.2 equiv) in ethanol (50 mL) was stirred under reflux for about 12 h. The reaction mixture was cooled to 0−10 °C, filtered, and dried for 6 h. It was further recrystallized by the DMF−DMSO mixture to afford the pure titled target compounds.[35] Purity of the synthesized compounds was in the range of 95−99%.

***N*′-(4-Chlorobenzylidene)-5-methyl-2-(pyridin-3-yl)-thiazole-4-carbohydrazide (5a).** Yellow solid; Yield: 82%; mp > 300 °C; FT-IR (KBr cm^{-1}): 3270 (N−H), 3041 (Ar−H), 2964 (C−H), 1665 (NH−CO), 1610 (C═N), 653 (C−S−C); ^{1}H NMR (DMSO-d_6, 400 MHz): δ 2.48 (s, 3H, thz-CH_3), 7.38−7.33 (d, 2H, Ar−H, J = 7.8 Hz), 7.60−7.57 (m, 1H, Pyr-H), 7.85 (d, 2H, Ar−H, J = 7.8 Hz), 8.14 (s, 1H, ═CH), 8.39 (d, 1H, Pyr-H, J = 7.2 Hz), 8.73 (d, 1H, Pyr-H, J = 4 Hz), 9.21 (s, 1H, Pyr-H), 11.95 (s, 1H, N−H); ^{13}C NMR (DMSO-d_6, 100 MHz): δ 15.2, 115.4, 115.6, 127.5, 130.3, 130.4, 130.7, 131.1, 134.5, 134.9, 149.3, 151.4, 155.7, 157.2, 160.2, 162.3, 168.5; LCMS (m/z): 357.05 $[M + H]^+$, 359.32 $[(M + 2) + H]^+$; Elemental analysis of $C_{17}H_{13}N_4ClOS$ Calcd: C, 57.22; H, 3.67; N, 15.70. Found: C, 57.20; H, 3.65; N, 15.72.

***N*′-(3,4-Dimethoxybenzylidene)-5-methyl-2-(pyridin-3-yl)thiazole-4-carbohydrazide (5b).** Pale yellow solid; Yield: 80%; mp 230−232 °C; FT-IR (KBr cm^{-1}): 3447 (N−H), 3014 (Ar−H), 2839 (C−H), 1648 (−NHCO), 1597 (C═N), 651 (C−S−C); ^{1}H NMR (DMSO-d_6, 400 MHz): δ 2.79 (s, 3H, thz-CH_3), 3.81 (s, 3H,−OCH_3), 3.85 (s, 3H, −OCH_3), 7.04 (d, 1H, Ar−H, J = 8.4 Hz), 7.21−7.23 (m, 1H, Ar−H), 7.45 (s, 1H, Ar−H), 7.56−7.59 (m, 1H, Pyr-H), 8.03 (s, 1H, ═CH), 8.32 (d, 1H, Pyr-H, J = 8 Hz), 8.71 (d, 1H, Pyr-H, J = 4 Hz), 9.14 (s, 1H, Pyr-H), 11.80 (s, 1H, −NH); ^{13}C NMR (DMSO-d_6, 100 MHz): δ 15.2, 56.8, 110.1, 114.1, 122.1, 127.5, 129.4, 131.1, 134.5, 134.9, 148.6, 149.3, 149.8, 150.5, 151.4, 155.7, 157.2, 168.5, 181.7; LCMS (m/z): 383.10 $[M + H]^+$; Elemental analysis of $C_{19}H_{18}N_4O_3S$ Calcd: C, 59.67; H, 4.74; N, 14.65. Found: C, 59.65; H, 4.75; N, 14.63.

5-Methyl-*N*′-(3-nitrobenzylidene)-2-(pyridin-3-yl)-thiazole-4-carbohydrazide (5c). Yellow solid; Yield: 75%; mp 266−268 °C; FT-IR (KBr cm^{-1}): 3440 (N−H), 3041 (Ar−H), 2868 (C−H), 1651 (−NHCO), 1609 (C═N), 650 (C−S−C); ^{1}H NMR (DMSO-d_6, 400 MHz): δ 2.69 (s, 3H, thz-CH_3), 7.56−7.59 (m, 1H, Pyr-H), 7.78 (d, 1H, Ar−H, J = 7.2 Hz), 8.04 (d, 1H, Ar−H, J = 7.6 Hz), 8.23 (d, 1H, Ar−H, J = 7.6 Hz), 8.35 (s, 1H, ═CH), 8.4 (s, 1H, Ar−H), 8.42 (d,

https://dx.doi.org/10.1021/acsomega.0c03386
ACS Omega 2020, 5, 25228−25239

1H, Pyr-H, J = 8 Hz), 8.75 (d, 1H, Pyr-H, J = 4 Hz), 9.24 (s, 1H, Pyr-H), 11.75 (s, 1H, −NH); ^{13}C NMR (DMSO-d_6, 100 MHz): δ 53.6, 107.1, 110.6, 120.1, 123.2, 125.1, 135.7, 144.7, 149.0, 150.5, 160.1, 160.8, 172.5; LCMS (m/z): 368.23 [M + H]$^+$; Elemental analysis for $C_{17}H_{13}N_5O_3S$ Calcd: C, 55.58; H, 3.57; N, 19.06. Found: C, 55.60; H, 3.60; N, 19.05.

5-Methyl-*N*′-(4-methylbenzylidene)-2-(pyridin-3-yl)-thiazole-4-carbohydrazide (5d). Yellow solid; Yield: 85%; mp 216−218 °C; FT-IR (KBr cm^{-1}): 3444 (N−H), 3049 (Ar−H), 2861 (C−H), 1655 (−NHCO), 1605 (C═N), 652 (C−S−C); ^{1}H NMR (DMSO-d_6, 400 MHz): δ 2.43 (s, 3H, CH_3), 2.61 (s, 3H, thz-CH_3), 7.32 (d, 2H, Ar−H, J = 7.8 Hz), 7.52−7.55 (m, 1H, Pyr-H), 7.76 (d, 2H, Ar−H, J = 7.8 Hz), 8.01 (s, 1H, ═CH), 8.1 (d, 1H, Pyr-H, J = 7.8 Hz), 8.70 (d, 1H, Pyr-H, J = 4.6 Hz), 9.24 (s, 1H, Pyr-H), 11.72 (s, 1H, N−H); ^{13}C NMR (DMSO-d_6, 100 MHz): δ 28.1, 54.2, 108.3, 110.5, 123.1, 124.2, 126.5, 134.2, 146.8, 148.9, 152.6, 161.6, 174.2; LCMS (m/z): 337.42 [M + H]$^+$; Elemental analysis for $C_{18}H_{16}N_4OS$ Calcd: C, 64.27; H, 4.79; N, 16.65. Found: C, 64.25; H, 4.80; N, 16.63.

***N*′-[(furan-2-ylmethylidene)-5-methyl]-2-(pyridin-3-yl)thiazole-4-carbohydrazide (5e).** Yellow solid; Yield: 68%; mp 120−122 °C; FT-IR (KBr cm^{-1}): 3434 (N−H), 3040 (Ar−H), 2860 (C−H), 1635 (−NHCO), 1609 (C═N), 658 (C−S−C); ^{1}H NMR (DMSO-d_6, 400 MHz): δ 2.62 (s, 3H, thz-CH_3), 6.53 (t, 1H, furan-H, J = 3.6 Hz), 7.29 (d, 1H, furan-H, J = 3.6 Hz), 7.44−7.47 (m, 1H, Pyr-H), 7.65 (d, 1H, furan-H, of J = 1.8 Hz), 7.85 (s, 1H, ═CH), 8.22 (d, 1H, Pyr-H, J = 7.4 Hz), 8.68 (d, 1H, Pyr-H, J = 4.7 Hz), 9.18 (s, 1H, Pyr-H), 11.12 (s, 1H, N−H); ^{13}C NMR (DMSO-d_6, 100 MHz): δ 55.5, 108.0, 111.8, 120.9, 124.3, 126.4, 134.3, 147.3, 149.1, 151.6, 160.1, 175.3; LCMS (m/z): 313.35 [M + H]$^+$; Elemental analysis for $C_{15}H_{12}N_4O_2S$ Calcd: C, 57.68; H, 3.87; N, 17.94. Found: C, 57.69; H, 3.88; N, 17.95.

***N*′-(3,4-Dimethylbenzylidene)-5-methyl-2-(pyridin-3-yl)thiazole-4-carbohydrazide (5f).** Pale yellow solid; Yield: 82%; mp 210−212 °C; FT-IR (KBr cm^{-1}): 3445 (N−H), 3024 (Ar−H), 2865 (C−H), 1621 (−NHCO), 1618 (C═N), 659 (C−S−C); ^{1}H NMR (DMSO-d_6, 400 MHz): δ 2.28 (s, 3H, $-CH_3$), 2.31 (s, 3H, $-CH_3$), 2.56 (s, 3H, thz-CH_3), 7.01 (d, 1H, Ar−H, J = 8.4 Hz), 7.18−7.21 (m, 1H, Ar−H), 7.38 (s, 1H, Ar−H), 7.56−7.58 (m, 1H, Pyr-H), 8.01 (s, 1H, ═CH), 8.30 (d, 1H, Pyr-H, J = 8 Hz), 8.68 (d, 1H, Pyr-H, J = 4 Hz), 9.13 (s, 1H, Pyr-H), 11.78 (s, 1H, −NH); ^{13}C NMR (DMSO-d_6, 100 MHz): δ 28.1, 54.5, 107.5, 110.8, 121.0, 123.4, 126.7, 134.5, 146.8, 148.1, 151.4, 161.5, 175.2; LCMS (m/z): 351.28 [M]$^+$; Elemental analysis for $C_{19}H_{18}N_4OS$ Calcd: C, 65.12; H, 5.18; N, 15.99. Found: C, 65.10; H, 5.16; N, 15.97.

***N*′-(4-(Benzyloxy)benzylidene)-5-methyl-2-(pyridin-3-yl)thiazole-4-carbohydrazide (5g).** Yellow solid; Yield: 70%; mp 208−210 °C; FT-IR (KBr cm^{-1}): 3432 (N−H), 3073 (Ar−H), 2866 (C−H), 1653 (−NHCO), 1622 (C═N), 648 (C−S−C); ^{1}H NMR (DMSO-d_6, 400 MHz): δ 2.63 (s, 3H, thz-CH_3), 5.16 (s, 2H, CH_2), 7.18 (d, 2H, Ar−H, J = 7.8 Hz), 7.36 (m, 1H, Ar−H), 7.38 (d, 2H, Ar−H, J = 7.7 Hz), 7.47 (d, 2H, Ar−H, J = 7.7 Hz), 7.53−7.56 (m, 1H, Pyr-H), 7.87 (d, 2H, Ar−H, J = 7.8 Hz), 8.02 (s, 1H, ═CH), 8.11 (d, 1H, Pyr-H, J = 7.6 Hz), 8.71 (d, 1H, Pyr-H, J = 4.6 Hz), 9.25 (s, 1H, Pyr-H), 11.73 (s, 1H, N−H); ^{13}C NMR (DMSO-d_6, 100 MHz): δ 55.6, 70.9, 108.3, 111.5, 114.8, 120.1, 124.4, 126.6, 127.1, 127.6, 128.9, 132.3, 133.7, 136.7, 146.8, 149.0, 151.5, 161.8, 164.8, 176.6; LCMS (m/z): 429.51 [M + H]$^+$; Elemental analysis for $C_{24}H_{20}N_4O_2S$ Calcd: C, 67.27; H, 4.70; N, 13.08. Found: C, 67.25; H, 4.72; N, 13.09.

***N*′-(4-Dimethylaminobenzylidene)-5-methyl-2-(pyridine-3-yl)thiazole-4-carbohydrazide (5h).** Yellow solid; Yield: 81%; mp 212−214 °C; FT-IR (KBr cm^{-1}): 3435 (N−H), 3043 (Ar−H), 2849 (C−H), 1654 (−NHCO), 1610 (C═N), 653 (C−S−C); ^{1}HNMR (DMSO-d_6, 400 MHz): δ 2.79 (s, 3H, thz-CH_3), 2.99 (s, 6H, N−Me), 6.81 (d, 1H, Ar−H, J = 8.8 Hz), 7.6 (d, 4H, Ar−H, J = 8.4 Hz), 8.0 (s, 1H, ═CH), 8.39 (d, 1H, Pyr-H, J = 8.4 Hz), 8.73 (d, 1H, Pyr-H, J = 4.4 Hz), 9.19 (s, 1H, Pyr-H), 11.66 (s, 1H, N−H); ^{13}C NMR (DMSO-d_6, 100 MHz): δ 19.3, 52.1, 112.5, 120.4, 121.6, 124.9, 129.2, 134.3, 145.4, 147.5, 151.9, 161.6, 161.8, 167.5; LCMS (m/z): 366.46 [M + H]$^+$; Elemental analysis for $C_{19}H_{19}N_5OS$ Calcd: C, 62.45; H, 5.24; N, 19.16. Found: C, 62.45; H, 5.25; N, 19.15.

***N*′-(4-Hydroxybenzylidene)-5-methyl-2-(pyridin-3-yl)thiazole-4-carbohydrazide (5i).** Yellow solid; Yield: 83%; mp above 300 °C; FT-IR (KBr cm^{-1}): 3434 (N−H), 2980 (Ar−H), 2832 (C−H), 1664 (−NHCO), 1615 (C═N), 641 (C−S−C); ^{1}H NMR (DMSO-d_6, 400 MHz): δ 2.65 (s, 3H, thz-CH_3), 7.21 (d, 2H, Ar−H, J = 8.2 Hz), 7.76−7.78 (m, 1H, Pyr-H), 7.82 (d, 2H, Ar−H, J = 8.2 Hz), 8.10 (s, 1H, ═CH), 8.42 (d, 1H, Pyr-H, J = 7.6 Hz), 8.72 (d, 1H, Pyr-H, J = 4.7 Hz), 9.15 (s, 1H, Pyr-H), 9.93 (s, 1H, O−H), 11.72 (s, 1H, N−H); ^{13}C NMR (DMSO-d_6, 100 MHz): δ 49.1, 112.3, 120.1, 121.3, 124.3, 129.1, 131.2, 133.1, 136.1, 146.7, 148.2, 151.3, 161.3, 171.6; LCMS (m/z): 339.39 [M + H]$^+$; Elemental analysis for $C_{17}H_{14}N_4O_2S$ Calcd: C, 60.34; H, 4.17; N, 16.56. Found: C, 60.32; H, 4.15; N, 16.57.

***N*′-(5-Bromo-2-hydroxybenzylidene)-5-methyl-2-(pyridin-3-yl)thiazole-4-carbohydrazide (5j).** Yellow solid; Yield: 78%; mp 258−260 °C; FT-IR (KBr cm^{-1}): 3432 (N−H), 2966 (Ar−H), 2866 (C−H), 1672 (−NHCO), 1612 (C═N), 651 (C−S−C); ^{1}H NMR (DMSO-d_6, 400 MHz): δ 2.69 (s, 3H, thz-CH_3), 6.99 (d, 1H, Ar−H, J = 8.4 Hz), 7.48 (d, 1H, Ar−H, J = 8.4 Hz), 7.78−7.80 (m, 1H, Pyr-H), 7.82 (s, 1H, Ar−H), 8.02 (s, 1H, ═CH), 8.19 (d, 1H, Pyr-H, J = 7.6 Hz), 8.68 (d, 1H, Pyr-H, J = 4.7 Hz), 9.20 (s, 1H, Pyr-H), 10.52 (s, 1H, O−H), 11.70 (s, 1H, N−H); ^{13}C NMR (DMSO-d_6, 100 MHz): δ 51.2, 112.8, 120.0, 120.6, 124.5, 129.5, 131.8, 133.3, 135.8, 146.6, 147.3, 152.3, 161.1, 170.6; LCMS (m/z): 418.28 [M + H]$^+$, 420.21 [(M + 2) + H]$^+$; Elemental analysis for $C_{17}H_{13}N_4BrO_2S$ Calcd: C, 48.93; H, 3.14; N, 13.43. Found: C, 48.91; H, 3.15; N, 13.44.

***N*′-[(1*H*-indol-3-yl)methylidene]-5-methyl-2-(pyridin-3-yl)thiazole-4-carbohydrazide (5k).** Yellow solid; Yield: 84%; mp above 300 °C; FT-IR (KBr cm^{-1}): 3438 (N−H), 2981 (Ar−H), 2866 (C−H), 1651 (−NHCO), 1614 (C═N), 658 (C−S−C); ^{1}H NMR (DMSO-d_6, 400 MHz): δ 2.62 (s, 3H, thz-CH_3), 7.04−7.14 (m, 2H, indolyl-H), 7.65 (m, 3H, indolyl-H), 7.79−7.81 (m, 1H, Pyr-H), 8.05 (s, 1H, ═CH), 8.22 (d, 1H, Pyr-H, J = 7.4 Hz), 8.68 (d, 1H, Pyr-H, J = 4.7 Hz), 9.18 (s, 1H, Pyr-H), 10.23 (s, 1H, indole N−H), 11.12 (s, 1H, N−H); ^{13}C NMR (DMSO-d_6, 100 MHz): δ 54.5, 108.0, 111.8, 116.3, 118.4, 120.2, 123.9, 124.4, 126.2, 128.1, 134.1, 147.7, 148.8, 152.2, 161.2, 175.5; LCMS (m/z): 362.42 [M + H]$^+$; Elemental analysis for $C_{19}H_{15}N_5OS$ Calcd: C, 63.14; H, 4.18; N, 19.38. Found: C, 61.90; H, 4.30; N, 20.03.

***N*′-(4-Hydroxy-3-methoxybenzylidene)-5-methyl-2-(pyridin-3-yl)thiazole-4-carbohydrazide (5l).** Yellow solid; Yield: 85%; mp 262−264 °C; FT-IR (KBr cm^{-1}): 3441 (N−H), 2975 (Ar−H), 2865 (C−H), 1672 (−NHCO),

https://dx.doi.org/10.1021/acsomega.0c03386
ACS Omega 2020, 5, 25228−25239

1619 (C═N), 655 (C−S−C); ^{1}H NMR (DMSO-d_6, 400 MHz): δ 2.76 (s, 3H, thz-CH_3), 3.83 (s, 3H, −OCH_3), 7.01 (m, 1H, Ar−H), 7.31−7.33 (m, 1H, Ar−H), 7.40 (s, 1H, Ar−H), 7.58−7.56 (m, 1H, Pyr-H), 8.08 (s, 1H, ═CH), 8.34 (d, 1H, Pyr-H, J = 8 Hz), 8.69 (d, 1H, Pyr-H, J = 4 Hz), 9.15 (s, 1H, Pyr-H), 9.65 (s, 1H, −OH), 11.82 (s, 1H, −NH); ^{13}C NMR (DMSO-d_6, 100 MHz): δ 50.9, 114.4, 120.2, 121.2, 124.9, 126.0, 129.9, 131.1, 133.1, 135.2, 146.5, 147.2, 151.4, 161.9, 171.7; LCMS (m/z): $[M + H]^+$; Elemental analysis for $C_{18}H_{16}N_4O_3S$ Calcd: C, 58.68; H, 4.38; N, 15.21. Found: C, 58.69; H, 4.40; N, 15.22.

Biological Activity. *In Vitro Anti-inflammatory Activity (Denaturation of the Bovine Serum Albumin Method).* The anti-inflammatory activity of the target compounds was determined by denaturation of the bovine serum albumin technique as per the Mizushima and Kobayashi[36] and Sakat *et al.*[37] reported method. The test sample contains the test compound and 1% aqueous solution of the bovine albumin fraction, and the pH of the reaction mixture was adjusted to pH 7.4 using suitable stripping solutions. Further, test samples were incubated at 37 °C for 20 min, and then, they was heated to 51 °C for 20 min. Later, it was cooled to ambient temperature, and the obtained turbidity of the sample was measured at 660 nm using a UV−visible spectrophotometer. The experiment was performed in triplicates using diclofenac sodium as the standard drug.

The anti-inflammatory activity of the titled compounds was estimated based on the percentage of inhibition of albumin denaturation using the following equation

$$\% \text{ inhibition} = \frac{[\text{control absorbance} - \text{sample absorbance}]}{\text{control absorbance}} \times 100$$

Antimicrobial Activity by the Macrodilution Broth Method. The antimicrobial susceptibility of the target compounds was evaluated by the NCCLS macrodilution broth method. The MIC of the target compounds was evaluated according to the Clinical and Laboratory Standards Institute (CLSI)[38] protocol. As the definition of the Clinical and Laboratory Standards Institute document[39] states, "the MIC is the lowest concentration of the antimicrobial agent that completely inhibits growth of the organism in the tubes or microdilution wells as detected by the unaided eye". Hence, the standard procedure was followed. Antimicrobial evaluation was carried out for the synthesized novel thiazole-based hydrazides against fungal strains such as *Aspergillus flavus* (*A. flavus*) (MTCC 1316), *Trichoderma atroviridae* (*T. atroviridae*) (MTCC 28036), *Penicillium citranum* (*P. citranum*) (MTCC 9849), *and Candida albicans* (*C. albicans*) (MTCC 461) and bacterial strains such as *Staphylococcus aureus* (*S. aureus*) (MTCC 9660), *Bacillus subtilis* (*B. subtilis*) (MTCC 441), *Escherichia coli* (*E. coli*) (MTCC 443), and *Pseudomonas aeruginosa* (*P. aeruginosa*) (MTCC 424) at varying concentrations (0.125−128 μg/mL). Nystatin and tetracycline were used as a standard drug for antifungal and antibacterial evaluation, respectively. Sterile test tubes containing the target compounds were placed in sterile Mueller Hinton broth (MHB) medium for bacteria and sterile Saboraud dextrose broth (SDB) for the fungi for which the test microorganisms were added. The MHB and SDB tubes with and without target compounds were used as the control. The MIC was detected as the lowest concentration of the target compound containing the tube showing no visible growth of the test microorganism. The experiment was performed in triplicates, and the data were analyzed by SPSS 20.0 software.

Statistical Analysis. Statistical analysis was carried out using SPSS software, version 20.0. The experiments were carried out in triplicates, and the data were expressed as mean ± standard deviation by one-way ANOVA. Turkey's multiple comparison test was used to determine significant differences between the standard and synthesized compounds. Correlation analysis was carried out using Pearson's correlation analysis using p = 0.01.

In Silico Prediction of Physicochemical and ADME Parameters. Physicochemical parameters of the designed compounds were predicted *in silico* using the QikProp module of Schrödinger. Various parameters predicted were molecular weight (M.Wt.), total solvent-accessible volume (TSAV), number of hydrogen bond donors (HBDs), number of hydrogen bond acceptors (HBAs), van der Waals polar surface area (PSA) of nitrogen and oxygen atoms, octanol/water partition coefficient (log P), aqueous solubility (log S), predicted Caco-2 cell permeability in nm/s (PCaco), apparent Madin Darby canine kidney (MDCK) permeability, and percentage of human oral absorption.[39−41] The details of the predicted values are presented in 5.

Molecular Docking Studies. Molecular docking of the significantly active compound was performed using the Glide module of Schrödinger software[42] installed on the Intel Xenon W3565 processor and Ubuntu enterprise version 14.04 as an operating system. The selected target protein structure was retrieved from the RCSB protein data bank.[43] The titled ligand was drawn using Chemdraw 18.0 PerkinElmer software.

Ligand Preparation. The ligands used as an input for the docking study was sketched by ChemDraw software, and the structure was cleaned up for bond alignment. Then, ligands were incorporated into the workstation, and the energy was minimized using the OPLS3e (Optimized Potentials for Liquid Simulations) force field in LigPrep[43] (version 2019-1, Schrödinger). This minimization helps to assign bond orders, addition of hydrogens to the ligands, and conversion of 2D to the 3D structure for the docking studies. The generated output file (best conformations of the ligands) was further used for docking studies.

Protein Preparation. The protein preparation wizard[44] (version 2019−1, Schrödinger) was the main tool in Schrödinger to prepare and minimize the protein. The hydrogen atom was added to the protein, and charges were assigned. Het states were generated using Epik at pH 7.0 ± 2.0. The protein was preprocessed and refined, and the protein was modified by analyzing the workspace water molecules and others. The critical water molecules remained the same, and the rest of the molecules apart from heteroatoms was deleted. Finally, the protein was minimized using the OPLS3 force field. A grid was created by considering the co-crystal ligand, which was included in the active site of the protein of the selected target (PDB-3LN1).[45] After the final step of docking with the co-crystal ligand in the XP mode, RMSD was checked to validate the protein, and the RMSD value was found to be 0.20 Å.

Receptor Grid Generation. A receptor grid was generated around the protein (PDB: 3LN1) by choosing the inhibitory ligand (X-ray pose of the ligand in the protein). The centroid of the ligand was selected to create a grid box around it, and the van der Waal radius of the receptor atoms was scaled to 1.00 Å with a partial atomic charge of 0.25.

https://dx.doi.org/10.1021/acsomega.0c03386
ACS Omega 2020, 5, 25228−25239

Docking Validation. The most straightforward way of validating the accuracy of specified parameters for docking studies is to redock the co-crystallized ligand back into the binding site of the protein and calculate the RMSD value between the crystallographic orientation and the docking pose. The calculation of RMSD is a convenient method to study how much a structure has diverged from its initial geometry. Lower RMSD value between its docked pose and crystallographic orientation is an indication of the suitability of the docking protocol. Therefore, before the screening of all ligands, the co-crystal structure of 3LN1 was chosen, and their inhibitor was redocked back to their active site. The RMSD value of the crystallographic orientation and the best docked pose was found to be 0.20 Å.[46,47]

Docking Analysis. Docking and analysis of molecular docking were performed using the above prepared ligand and protein as the input. The results of the docking study were analyzed with the help of the XP visualizer (Version 2019-1, Schrödinger). All docking calculations were performed using the extra precision (XP) mode. A scaling factor of 0.8 and a partial atomic charge of less than 0.15 were applied to the atoms of the protein. The glide docking score was used to determine the best docked confirmation from the output. The interactions of these docked conformations were investigated further using the XP visualizer, and the results are depicted in the tables (Tables 1 and 5) and pictures (Figures 6−10).

■ ASSOCIATED CONTENT

Supporting Information

The Supporting Information is available free of charge at https://pubs.acs.org/doi/10.1021/acsomega.0c03386.

FTIR, NMR (^{1}H and ^{13}C), and LCMS spectra of the specific compounds and graphical representations of results of the antibacterial and antifungal evaluation of the compounds (PDF)

■ AUTHOR INFORMATION

Corresponding Author

Boja Poojary − *Department of Post-Graduate Studies & Research in Chemistry, Mangalore University, Mangalagangothri 574199, Karnataka, India;* orcid.org/0000-0002-4977-3501; Phone: +91-824-2287262; Email: bojapoojary@gmail.com; Fax: +91-824-2287367/2287424

Authors

Vinuta Kamat − *Department of Post-Graduate Studies & Research in Chemistry, Mangalore University, Mangalagangothri 574199, Karnataka, India*

Rangappa Santosh − *Department of Post-Graduate Studies & Research in Chemistry, Mangalore University, Mangalagangothri 574199, Karnataka, India*

Suresh P. Nayak − *Department of Post-Graduate Studies & Research in Chemistry, Mangalore University, Mangalagangothri 574199, Karnataka, India*

Banoth Karan Kumar − *Medicinal Chemistry Research Laboratory, Department of Pharmacy, Birla Institute of Technology and Science, Pilani, Rajasthan 333031, India;* orcid.org/0000-0002-9615-6944

Murugesan Sankaranarayanan − *Medicinal Chemistry Research Laboratory, Department of Pharmacy, Birla Institute of Technology and Science, Pilani, Rajasthan 333031, India*

Faheem − *Medicinal Chemistry Research Laboratory, Department of Pharmacy, Birla Institute of Technology and Science, Pilani, Rajasthan 333031, India*

Sheela Khanapure − *Department of Biotechnology and Microbiology, Karnataka University, Dharwad 580003, Karnataka, India*

Delicia Avilla. Barretto − *Department of Biotechnology and Microbiology, Karnataka University, Dharwad 580003, Karnataka, India*

Shyam K. Vootla − *Department of Biotechnology and Microbiology, Karnataka University, Dharwad 580003, Karnataka, India*

Complete contact information is available at: https://pubs.acs.org/10.1021/acsomega.0c03386

Notes

The authors declare no competing financial interest.

■ ACKNOWLEDGMENTS

Author Vinuta Kamat would like to thank DST (Award letter No.: DST/KSTePS/Ph.D.Fellowship/CHE-05:2018-19 dated 08.03.2019) for providing fellowship. Author Banoth Karan Kumar would like to thank Ministry of Tribal Affairs, Government of India Award no-201920-NFST-TEL-01497). Authors M.S. and F.F. gratefully acknowledge BITS-Pilani for providing the necessary facilities to do this work. This work was carried out under a grant from the Department of Biotechnology Indo-Spain, New Delhi. (Ref. No: BT/IN/Spain/39/SM/2017−2018).

■ REFERENCES

(1) Lon, H.-K.; Liu, D.; Jusko, W. J. Pharmacokinetic/pharmacodynamic modeling in inflammation. *Crit. Rev. Biomed. Eng.* **2012**, *40*, 295−312.

(2) Sherwood, E. R.; Toliver-Kinsky, T. Mechanisms of the inflammatory response. *Best Pract. Res., Clin. Anaesthesiol.* **2004**, *18*, 385−405.

(3) Ferreira, S. H.; Vane, J. R. New aspects of the mode of action of nonsteroid anti-inflammatory drugs. *Annu. Rev. Pharmacol.* **1974**, *14*, 57−73.

(4) Vane, J. R. Inhibition of prostaglandin synthesis as a mechanism of action for aspirin-like drugs. *Nature, New Biol.* **1971**, *231*, 232−235.

(5) Jain, H. K.; Mourya, V. K.; Agrawal, R. K. Inhibitory mode of 2-acetoxyphenyl alkyl sulfides against COX-1 and COX-2: QSAR analyses. *Bioorg. Med. Chem. Lett.* **2006**, *16*, 5280−5284.

(6) Anana, R.; Rao, P. N. P.; Chen, Q.-H.; Knaus, E. E. Synthesis and biological evaluation of linear phenylethynylbenzenesulfonamide regioisomers as cyclooxygenase-1/-2 (COX-1/-2) inhibitors. *Bioorg. Med. Chem.* **2006**, *14*, 5259−5265.

(7) Kovala-Demertzi, D. Recent advances on non-steroidal anti-inflammatory drugs, NSAIDs: organotin complexes of NSAIDs. *J. Organomet. Chem.* **2006**, *691*, 1767−1774.

(8) Tacconelli, S.; Capone, M. L.; Sciulli, M. G.; Ricciotti, E.; Patrignani, P. The biochemical selectivity of novel COX-2 inhibitors in whole blood assays of COX-isozyme activity. *Curr. Med. Res. Opin.* **2002**, *18*, 503−511.

(9) Tiwari, A. D.; Panda, S. S.; Girgis, A. S.; Sahu, S.; George, R. F.; Srour, A. M.; Starza, B. L.; Asiri, A. M.; Hall, C. D.; Katritzky, A. R. Microwave assisted synthesis and QSAR study of novel NSAID acetaminophen conjugates with amino acid linkers. *Org. Biomol. Chem.* **2014**, *12*, 7238−7249.

(10) Morigi, R.; Locatelli, A.; Leoni, A.; Rambaldi, M. Recent patents on thiazole derivatives endowed with antitumor activity. *Recent Pat. Anti-Cancer Drug Discovery* **2015**, *10*, 280−297.

(11) Ghorab, M. M.; Al-Said, M. S. Antitumor activity of novel pyridine, thiophene and thiazole derivatives. *Arch. Pharmacal Res.* **2012**, *35*, 965−973.
(12) Jadhavar, S. C.; Bhansali, S. G.; Patwari, S. B.; Bhusare, S. R.; Kasralikar, H. M. Design, synthesis and docking studies of novel 1, 2, 3-triazolyl phenylthiazole analogs as potent anti-HIV-1 NNRT inhibitors. *Med. Chem.* **2017**, *7*, 268−275.
(13) Amr, A. E.-G. E.; Sabrry, N. M.; Abdalla, M. M.; Abdel-Wahab, B. F. Synthesis, antiarrhythmic and anticoagulant activities of novel thiazolo derivatives from methyl 2-(thiazol-2-ylcarbamoyl) acetate. *Eur. J. Med. Chem.* **2009**, *44*, 725−735.
(14) Maghraby, M. T.-E.; Abou-Ghadir, O. M. F.; Abdel-Moty, S. G.; Ali, A. Y.; Salem, O. I. A. Novel class of benzimidazole-thiazole hybrids: The privileged scaffolds of potent anti-inflammatory activity with dual inhibition of cyclooxygenase and 15-lipoxygenase enzymes. *Bioorg. Med. Chem.* **2020**, *28*, 115403.
(15) Ruberte, A. C.; Ramos-Inza, S.; Aydillo, C.; Talavera, I.; Encío, I.; Plano, D.; Sanmartín, C. Novel *N, N′*-disubstituted acylselenoureas as potential antioxidant and cytotoxic agents. *Antioxidants* **2020**, *9*, 55.
(16) Ghonim, A. E.; Ligresti, A.; Rabbito, A.; Mahmoud, A. M.; Di Marzo, V.; Osman, N. A.; Abadi, A. H. Structure-activity relationships of thiazole and benzothiazole derivatives as selective cannabinoid CB2 agonists with *in vivo* anti-inflammatory properties. *Eur. J. Med. Chem.* **2019**, *180*, 154−170.
(17) Hassan, F. A. Synthesis, characterization, anti-inflammatory, and antioxidant activities of some new thiazole derivatives. *Int. J. Sci. Tech.* **2012**, *2*, 180−187.
(18) Iyer, V. B.; Gurupadayya, B.; Koganti, V. S.; Inturi, B.; Chandan, R. S. Design, synthesis and biological evaluation of 1, 3, 4-oxadiazoles as promising anti-inflammatory agents. *Med. Chem. Res.* **2017**, *26*, 190−204.
(19) Mahmoud, H. K.; Abbas, A. A.; Gomha, S. M. Synthesis, antimicrobial evaluation and molecular docking of new functionalized bis (1, 3, 4-thiadiazole) and bis (thiazole) derivatives. *Polycyclic Aromat. Compd.* **2020**, *7*, 1−13.
(20) Adole, V. A.; More, R. A.; Jagdale, B. S.; Pawar, T. B.; Chobe, S. S. Efficient synthesis, antibacterial, antifungal, antioxidant and cytotoxicity study of 2-(2-hydrazineyl) thiazole derivatives. *ChemistrySelect* **2020**, *5*, 2778−2786.
(21) Wang, L.-L.; Battini, N.; Bheemanaboina, R. R. Y.; Zhang, S.-L.; Zhou, C.-H. Design and synthesis of aminothiazolyl norfloxacin analogues as potential antimicrobial agents and their biological evaluation. *Eur. J. Med. Chem.* **2019**, *167*, 105−123.
(22) Eryılmaz, S.; Çelikoğlu, E. T.; İdil, Ö.; İnkaya, E.; Kozak, Z.; Mısır, E.; Gül, M. Derivatives of pyridine and thiazole hybrid: Synthesis, DFT, biological evaluation *via* antimicrobial and DNA cleavage activity. *Bioorg. Chem.* **2020**, *95*, 103476.
(23) Fan, Z.; Shi, J.; Luo, N.; Ding, M.; Bao, X. Synthesis, crystal structure, and agricultural antimicrobial evaluation of novel quinazoline thioether derivatives incorporating the 1, 2, 4-triazolo [4, 3-*a*] pyridine moiety. *J. Agric. Food Chem.* **2019**, *67*, 11598−11606.
(24) Bhila, V. G.; Patel, C. V.; Patel, N. H.; Brahmbhatt, D. I. One pot synthesis of some novel coumarins containing 5-(substituted-2-hydroxybenzoyl) pyridine as a new class of antimicrobial and antituberculosis agents. *Med. Chem. Res.* **2013**, *22*, 4338−4346.
(25) Desai, N. C.; Bhatt, N. B.; Joshi, S. B.; Jadeja, K. A.; Khedkar, V. M. Synthesis, antimicrobial activity and 3D-QSAR study of hybrid oxazine clubbed pyridine scaffolds. *ChemistrySelect* **2019**, *4*, 7541−7550.
(26) Rani, V. E.; Reddy, P. R. Synthesis and antimicrobial activity of new pyridine containing substituted phenyl azetidine-2-one derivatives. *Open J. Med. Chem.* **2018**, *08*, 22−29.
(27) Rashdan, H. R. M.; Abdel-Aziem, A.; El-Naggar, D. H.; Nabil, S. Synthesis and biological evaluation of some new pyridines, isoxazoles and isoxazolopyridazines bearing 1, 2, 3-triazole moiety. *Acta Pol. Pharm.* **2019**, *76*, 469−482.
(28) Laddha, S. S.; Bhatnagar, S. P. A new therapeutic approach in Parkinson's disease: Some novel quinazoline derivatives as dual selective phosphodiesterase 1 inhibitors and anti-inflammatory agents. *Bioorg. Med. Chem.* **2009**, *17*, 6796−6802.
(29) Kumar, N.; Chauhan, A.; Drabu, S. Synthesis of cyanopyridine and pyrimidine analogues as new anti-inflammatory and antimicrobial agents. *Biomed. Pharmacother.* **2011**, *65*, 375−380.
(30) Thirumurugan, P.; Mahalaxmi, S.; Perumal, P. T. Synthesis and anti-inflammatory activity of 3-indolyl pyridine derivatives through one-pot multi component reaction. *J. Chem. Sci.* **2010**, *122*, 819−832.
(31) (a) Liu, H.; Long, S.; Rakesh, K. P.; Zha, G.-F. Structure-activity relationships (SAR) of triazine derivatives: Promising antimicrobial agents. *Eur. J. Med. Chem.* **2020**, *185*, 111804. (b) Rakesh, K. P.; Kumara, H. K.; Ullas, B. J.; Shivakumara, J.; Channe Gowda, D. Amino acids conjugated quinazolinone-Schiff's bases as potential antimicrobial agents: Synthesis, SAR and molecular docking studies. *Bioorg. Chem.* **2019**, *90*, 103093. (c) Xu, M.; Wu, P.; Shen, F.; Ji, J.; Rakesh, K. P. Chalcone derivatives and their antibacterial activities: current development. *Bioorg. Chem.* **2019**, *91*, 103133. (d) Rakesh, K. P.; Gowda, D. C. Schiff's bases of quinazolinone derivatives: Synthesis and SAR studies of a novel series of potential anti-inflammatory and antioxidants. *Bioorg. Med. Chem. Lett.* **2015**, *25*, 1072−1077. (e) Rakesh, K. P.; Ramesh, S.; Kumar, H. M.; Chandan, S.; Gowda, D. C. Quinazolinones linked amino acids derivatives as a new class of promising antimicrobial, antioxidant and anti-inflammatory agents. *Eur. J. Chem.* **2015**, *6*, 254−260. (f) Rakesh, K. P.; Gowda, D. C.; Gowda, D. C. Anti-inflammatory and antioxidant peptide-conjugates: Modulation of activity by charged and hydrophobic residues. *Int. J. Pept. Res. Ther.* **2019**, *25*, 227−234. (g) Rakesh, K. P.; Shivakumar, S.; Gowda, D. C. Effect of low charge and high hydrophobicity on antimicrobial activity of the quinazolinone-peptide conjugates. *Russ. J. Bioorg. Chem.* **2018**, *44*, 158−164. (h) Rakesh, K. P.; Sridhara, M. B.; Manukumar, H. M.; Qin, H.-L.; Qin, H. L. Benzisoxazole: A privileged scaffold for medicinal chemistry. *MedChemComm* **2017**, *8*, 2023−2039. (i) Manukumar, H. M.; Chandrasekhar, B.; Rakesh, K. P.; Ananda, A. P.; Nandhini, M.; Lalitha, P.; Sumathi, S.; Qin, H.-L.; Umesha, S. Novel TC@ AgNPs mediated biocidal mechanism against biofilm associated methicillin-resistant Staphylococcus aureus (Bap-MRSA) 090, cytotoxicity and its molecular docking studies. *MedChemComm* **2017**, *8*, 2181−2194.
(32) Kaboudin, B.; Elhamifar, D. Phosphorus pentasulfide: A mild and versatile reagent for the preparation of thioamides from nitriles. *Synth* **2006**, *2006*, 224−226.
(33) Ali, M. R.; Kumar, S.; Afzal, O.; Shalmali, N.; Sharma, M.; Bawa, S. Development of 2-(substituted benzylamino)-4-methyl-1, 3-thiazole-5-carboxylic acid derivatives as xanthine oxidase inhibitors and free radical scavengers. *Chem. Biol. Drug Des.* **2016**, *87*, 508−516.
(34) Han, M. İ.; Bekçi, H.; Uba, A. I.; Yıldırım, Y.; Karasulu, E.; Cumaoğlu, A.; Karasulu, H. Y.; Yelekçi, K.; Yılmaz, Ö.; Küçükgüzel, Ş. G. Synthesis, molecular modeling, *in vivo* study, and anticancer activity of 1, 2, 4-triazole containing hydrazide−hydrazones derived from (*S*)-naproxen. *Arch. Pharm.* **2019**, *352*, 1800365.
(35) Sıcak, Y.; Oruç-Emre, E. E.; Öztürk, M.; Taşkın-Tok, T.; Karaküçük-Iyidoğan, A. Novel fluorine-containing chiral hydrazide-hydrazones: Design, synthesis, structural elucidation, antioxidant and anticholinesterase activity and *in silico* studies. *Chirality* **2019**, *31*, 603−615.
(36) Mizushima, Y.; Kobayashi, M. Interaction of anti-inflammatory drugs with serum proteins, especially with some biologically active proteins. *J. Pharm. Pharmacol.* **1968**, *20*, 169−173.
(37) Sakat, S.; Juvekar, A. R.; Gambhire, M. N. *In vitro* antioxidant and anti-inflammatory activity of methanol extract of Oxalis corniculata Linn. *Int. J. Pharm. Pharm. Sci.* **2010**, *2*, 146−155.
(38) National Committee for Clinical Laboratory Standards. *Methods for Dilution Antimicrobial Susceptibility Tests for Bacteria that Grow Aerobically*. Approved standard, 7th ed.; NCCLS: Villanova PA, USA, 2006 http://demo.nextlab.ir/getattachment/737fedd6-3926-4099-b6c8-19aa279bfd1f/CLSI-M7-A7.aspx.
(39) Clinical and Laboratory Standards Institute. *Methods for Dilution Antimicrobial Susceptibility Tests for Bacteria that Grow*

https://dx.doi.org/10.1021/acsomega.0c03386
ACS Omega 2020, 5, 25228−25239

Aerobically; Approved Standard, 9th ed.; CLSI document M07-A9, 2012.
(40) van de Waterbeemd, H.; Gifford, E. ADMET *in silico* modelling: Towards prediction paradise. *Nat. Rev. Drug Discovery* **2003**, *2*, 192−204.
(41) *QikProp Descriptors and properties PISA*, 2015; pp 2−4.
(42) Chander, S.; Wang, P.; Ashok, P.; Yang, L.-M.; Zheng, Y.-T.; Sankaranarayanan, M. Design, synthesis and anti-HIV-1 RT evaluation of 2-(benzyl(4-chlorophenyl)amino)-1-(piperazin-1-yl)-ethanone derivatives. *Bioorg. Med. Chem. Lett.* **2017**, *27*, 61−65.
(43) *Schrödinger Release 2019-1: Glide*; Schrödinger, LLC: New York, NY.(5), 2019 https://www.rcsb.org/.
(44) *Schrödinger Release 2019-1*; LigPrep, Schrödinger, LLC: New York, NY, 2019.
(45) *Schrödinger Release 2019-1: Schrödinger Suite 2019-1 Protein preparation Wizard*; Epik, Schrödinger, LLC, New York, NY, 2019.
(46) Wang, J. L.; Limburg, D.; Graneto, M. J.; Springer, J.; Hamper, J. R. B.; Liao, S.; Pawlitz, J. L.; Kurumbail, R. G.; Maziasz, T.; Talley, J. J.; Kiefer, J. R.; Carter, J. The novel benzopyran class of selective cyclooxygenase-2 inhibitors. Part 2: The second clinical candidate having a shorter and favorable human half-life. *Bioorg. Med. Chem. Lett.* **2010**, *20*, 7159−7163.
(47) Ganesan, M. S.; Raja, K. K.; Narasimhan, K.; Murugesan, S.; Kumar, B. K. Design, synthesis, α-amylase inhibition and *in silico* docking study of novel quinoline bearing proline derivatives. *J. Mol. Struct.* **2020**, *1208*, 127873.

https://dx.doi.org/10.1021/acsomega.0c03386
ACS Omega 2020, 5, 25228−25239